Journal of Tropical Resources and Sustainable Science
Website : http://journal.umk.edu.my/index.php/jtrss/
eISSN : 2462-2389
Vol: 14 Issue 3, 2026, 800-810
DOI: https://doi.org/10.47253/jtrss.v14i3.2534

RESEARCH ARTICLE

Utilization of Riau peat-derived humic acid modified with urea-formaldehyde for Ni(II) adsorption: a geochemical approach

Meidita Kemala Sari[1,2*], Bambang Rusdiarso[1] and Sri Hilma Siregar[2]

[1]Department of Chemistry, Faculty of Mathematics and Natural Science, Universitas Gadjah Mada, Sekip Utara, PO BOX BLS 21, Yogyakarta 55281
[2]Department of Chemistry, Universitas Muhammadiyah Riau, Jalan Tuanku Tambusai, Delima, Tampan, Pekanbaru, Riau 28290

ARTICLE HISTORY
Received : 8 November 2025
Accepted : 30 December 2025
Online : 30 September 2026

KEYWORDS
humic acid,
urea-formaldehyde,
Ni(II) removal,
ionic strength effect,
adsorption.

☒ * **CORRESPONDING AUTHOR**
Meidita Kemala Sari
Universitas Muhammadiyah Riau
Email: meiditakemalasari@umri.ac.id

ABSTRACT

Nickel contamination in aquatic systems presents serious environmental and geochemical concerns due to its mobility, persistence, and toxicity. This study proposes a geochemically driven approach to develop a nitrogen enriched humic acid based adsorbent modified with urea formaldehyde (HA-UF) to enhance the removal of Ni(II) from aqueous solutions. Humic acid was extracted using an alkaline method and subsequently crosslinked with urea-formaldehyde through a one-step reflux process. The novelty of this study lies in the use of urea-formaldehyde (UF) as a stabilizing agent and in evaluating the effect of ionic strength on Ni(II) adsorption. The characteristic peaks of HA-UF confirmed the formation of C–O–C and C–N functional groups at 1035, 1136, and 1248 cm^{-1} (ATR-IR), semi-crystalline features at 2θ = 22° and 25° (XRD), and a substantial increase in nitrogen content from 6.85% to 23.46% (EDX). The HA-UF demonstrated enhanced stability (up to pH 12) and exhibited active functional groups (–COOH, –OH, –NH) that are conducive to binding Ni(II), while maintaining improved structural integrity and reduced total acidity. The adsorption process followed the Langmuir isotherm model, with the adsorption capacity increasing from 1.899 × 10^{-4} mol/g for HA to 3.682 × 10^{-4} mol/g for HA-UF, indicating a greater availability of active sites after modification. Kinetic analysis showed that the process followed a pseudo second order model, with a rate constant of 2.328 × 10^{-2} g/mol·min, suggesting that chemisorption occurred through surface complexation and ion-exchange mechanisms. The calculated adsorption energies (~20–22 kJ mol^{-1}) indicate intermediate-strength interactions dominated by coordination bonding rather than simple physisorption. Increasing ionic strength (NaCl) reduced both the adsorption capacity and rate, likely due to cation competition and compression of the electrical double layer. Overall, HA-UF exhibits reactivity comparable to natural organic matter while providing enhanced structural stability and adsorption performance, highlighting its potential application in wastewater treatment systems under variable pH and ionic strength conditions.

© 2026 UMK Publisher. All rights reserved.

1. INTRODUCTION

Nickel (Ni) contamination in aquatic environments is primarily caused by discharges from electroplating operations, mining effluents, and agro-industrial wastewaters, such as palm oil mill effluent (POME). Chronic exposure to Ni^{2+} has been linked to allergic reactions, renal and cardiovascular toxicity, and carcinogenic effects. Accordingly, the World Health Organization recommends a maximum Ni concentration of 0.07 mg/L in drinking water (Charazińska, Burszta-Adamiak, and Lochyński 2022; Genchi et al. 2020).

Humic acid (HA), a fraction of natural organic matter that is abundant in peat soils (Stevenson 1994), contains a diverse range of functional groups (–COOH, –OH, and phenolic groups) that confer a strong affinity for metal cations (Basuki et al. 2021a; Charazińska, Lochyński, and Burszta-Adamiak 2021; Isakov 2021). HA extracted from peat has demonstrated the ability to adsorb Ni(II), Cd(II), and Pb(II) efficiently (Basuki, Santosa, and Rusdiarso 2017; Rusdiarso and Basuki 2020), with adsorption kinetics often fitting a pseudo-second-order model and equilibrium behavior described by the Langmuir isotherm. The macromolecular structure of HA provides both ion-exchange sites and coordination interactions, making it a promising green adsorbent for heavy metal removal (Spark, Wells, and Johnson 1997; Xue et al. 2024).

To enhance the structural stability and metal binding capacity of HA, chemical crosslinking with urea formaldehyde (UF) has been explored (Ohalete and Popoola 2019; Sari, Basuki, and Rusdiarso 2021). Another study used

glutaraldehye (GA) as a chemical crosslinker. This GA modification significantly enhances HA's stability across a wider pH range, maintaining its structural integrity from pH 2 to 12. It also introduces additional binding sites (–C=N–), resulting in substantially improved Ni(II) adsorption capacities compared to unmodified HA (Santoso et al. 2010).

Understanding Ni(II) uptake mechanisms and the influence of solution chemistry relies on conventional adsorption isotherms and kinetic modeling (Charazińska et al. 2022; Liang et al. 2021; Sari and Rusdiarso 2022). In this study, the equilibrium data were fitted to the Langmuir and Freundlich isotherm models, while the adsorption kinetics were analyzed using pseudo-first-order and pseudo second order models under varying ionic strength and pH conditions. By comparing the model parameters in the presence and absence of competing ions, we aim to determine how ionic competition affects active site availability and overall adsorption performance. This insight will be invaluable for guiding the practical application of HA-UF adsorbents in real-world wastewater treatment.

Indonesia's peatlands store vast carbon stocks but have been extensively degraded by drainage, agricultural conversion, and recurrent fires. Valorizing degraded peat through the extraction of HA for HA-UF production aligns with national restoration policies and contributes to the Sustainable Development Goals (SDGs), particularly SDG 6 (Clean Water and Sanitation), SDG 12 (Responsible Consumption and Production), and SDG 13 (Climate Action). This approach integrates wastewater treatment with circular economy principles while promoting carbon sequestration co-benefits. Collectively, this geochemical approach to synthesizing and modeling HA-UF adsorbents from peat-derived HA offers a scalable, eco-friendly solution for Ni(II) remediation, bridging fundamental mechanistic insights with regional environmental and socioeconomic strategies.

2. MATERIALS AND METHODS

2.1. Materials

The humic acid used in this study was extracted from degraded peat soil collected in Bayas Jaya, Indragiri Hilir, Riau. All chemicals were of analytical grade and purchased from E. Merck (Germany), including NaOH, HCl, HF, and urea. A 37% (v/v) formaldehyde solution was used for crosslinking, $Ni(CH_3COO)_2 \cdot 2H_2O$ served as the Ni(II) source, and NaCl was used to adjust the ionic strength.

2.2. Synthesis and characterization of HA-UF

Humic acid was extracted from air-dried peat soil using a modified Stevenson (1994) method. The soil was mixed with 0.1 M NaOH (1:10 w/v) and stirred for 24 hours, then filtered and acidified to pH 1 with HCl to precipitate humic acid. The crude humic acid was collected and dried at 60 °C. Purification was carried out by soaking the crude product in a 1:1 mixture of 0.1 M HCl and 0.3 M HF for 24 hours, followed by centrifugation, washing, drying, and grinding to obtain purified humic acid (HA).

HA-UF was synthesized using a one-step reflux method at 75–80 °C. Urea (5 g) was mixed with 14 mL of 37% formaldehyde, then combined with 5 g of purified HA in 0.1 M NaOH. The mixture was refluxed for 4 hours and then neutralized with 2 M HCl, resulting in the formation of a precipitate. The HA-UF product was subsequently collected by centrifugation at 4000 rpm for 10 minutes and dried at 60 °C.

The HA-UF was then characterized using UV–Vis spectrophotometry (Shimadzu UV-1800, Japan), ATR-IR spectroscopy (Perkin Elmer, US), XRD (Bruker, Germany), and SEM-EDX analyses (JEOL JSM-6510LA, US), all conducted in Indonesia. HA-UF stability was tested by stirring 0.1 g of material in demineralized water at pH 1–14 for 24 hours.

2.3. Ni(II) adsorption by HA-UF

2.3.1 Effect of pH

Ni(II) solutions (50 mg/L; 50 mL) were adjusted to pH 2.2–10.3 using HCl or NaOH and then mixed with 50 mg of HA-UF. After 3 hours of stirring, the suspensions were filtered, and the residual Ni(II) concentration in the filtrate was determined using atomic absorption spectroscopy (AAS) (Perkin Elmer 3110, US).

2.3.2 Effect of ionic strength

Ni(II) solutions (50 mg/L, at the optimum pH) were mixed with 50 mg of HA-UF and NaCl (100–500 mg). After 3 hours of stirring, the suspensions were filtered, and the residual Ni(II) concentration in the filtrate was determined using atomic absorption spectroscopy (AAS) (Perkin Elmer 3110, US).

2.3.3 Adsorption capacity and ionic strength

Fifty milligrams of HA-UF were added to 50 mL of Ni(II) solutions (5–200 mg/L, at the optimum pH). After 3 hours of stirring, the suspensions were filtered, and the residual Ni(II) concentration in the filtrate was determined using atomic absorption spectroscopy (AAS) (Perkin Elmer 3110, US). Adsorption isotherms were determined using Langmuir and the Freundlich models. For ionic strength effects, NaCl (100–300 mg) was added, and results were compared with non-NaCl conditions.

 © 2026 UMK Publisher. All rights reserved.

2.3.4 Adsorption rate and ionic strength

Fifty milligrams of HA-UF was mixed with 50 mL of Ni(II) solution (120 mg/L) and agitated for varying contact times (10–180 minutes). After the designated contact time, the suspensions were filtered, and the residual Ni(II) concentration in the filtrate was determined using atomic absorption spectroscopy (AAS) (Perkin Elmer 3110, US). Adsorption kinetics were evaluated using pseudo first order and pseudo-second-order models. The same experimental procedure was followed, with the addition of NaCl (100–300 mg) to investigate the effect of ionic strength on sorption kinetics. Results were compared with those without NaCl to assess the impact of ionic strength.

2.4 Adsorption isotherm models

The Langmuir isotherm model describes adsorption on a homogeneous adsorbent surface with a finite number of identical active sites, no interactions between adsorbed species, and uniform adsorption until saturation. The Langmuir equation is expressed as:

$$q_e = \frac{K_L b C_e}{1 + b C_e} \qquad (1)$$

Where q_e(mol g^{-1}) is the amount of adsorbate adsorbed at equilibrium, b(mol g^{-1}) represents the maximum monolayer adsorption capacity, C_e(mol L^{-1}) is the equilibrium concentration of the adsorbate in solution, and K_L(L mol^{-1}) Is the Langmuir adsorption constant related to the affinity between the adsorbate and the adsorbent (Langmuir 1918).

A good fit to the Langmuir model indicates predominantly monolayer adsorption on a relatively uniform surface. For humic acid based adsorbents, this suggests that metal ions bind to specific functional groups (e.g., carboxylate, phenolic, or nitrogen-containing sites) until saturation is reached (Langmuir 1918; Sari et al. 2021).

The Freundlich isotherm is an empirical model describing adsorption on heterogeneous surfaces with non-uniform energies and possible multilayer formation, without assuming a finite adsorption capacity. The Freundlich equation is given as:

$$q_e = B C_e^{1/n} \qquad (2)$$

where B (mol g^{-1}) is the Freundlich constant related to adsorption capacity, and n It is the heterogeneity factor that reflects the favorability and intensity of adsorption. A value of $n > 1$ indicates favorable adsorption conditions (Freundlich 1907).

For both natural and modified humic substances, the Freundlich model accounts for surface heterogeneity, indicating adsorption on energetically diverse sites with varying affinities for metal ions (Freundlich 1907; Sari et al. 2021).

2.5 Adsorption kinetic models

The pseudo first order kinetic model assumes that the rate of adsorption is proportional to the number of unoccupied adsorption sites (Lagergren 1898; Wang and Guo 2020b). This model is generally applicable to physisorption-dominated processes and is expressed in its linear form as:

$$\ln(q_e - q_t) = \ln q_e - k_1 t \qquad (3)$$

where q_t(mol g^{-1}) is the amount of adsorbate adsorbed at time t, q_e(mol g^{-1}) is the adsorption capacity at equilibrium, and k_1(min^{-1}) is the pseudo-first-order rate constant. Although widely applied, this model often fails to accurately describe adsorption behavior over the entire contact time, particularly when chemisorption or surface complexation mechanisms dominate.

The pseudo-second-order kinetic model assumes that the adsorption rate is controlled by chemisorption involving valence forces such as electron sharing or exchange between the adsorbent and adsorbate. (Ho and McKay. G 1995; Wang and Guo 2020b). This model is expressed as:

$$\frac{t}{q_t} = \frac{1}{k_2 q_e^2} + \frac{t}{q_e} \qquad (4)$$

where k_2(g mol^{-1} min^{-1}) is the pseudo-second-order rate constant. This model is particularly suitable for systems in which adsorption is governed by chemical interactions, such as ion exchange, surface complexation, or coordination bonding. Strong agreement with the pseudo second order model indicates chemisorption-controlled kinetics; in humic acid based and nitrogen enriched adsorbents, this behavior is associated with metal binding through oxygen and nitrogen containing functional groups.

3. RESULT AND DISCUSSION

3.1 Characterization of HA-UF

The modification of humic acid (HA) with urea formaldehyde (UF) was confirmed using a combination of characterization techniques, including ATR-IR, XRD, SEM-EDX, total acidity analysis, and pH stability measurements.

In particular, comparison of the ATR-IR spectra of unmodified HA and UF-modified HA reveals several consistent changes attributable to UF incorporation (Figure 1). The broad band at 3300–3600 cm^{-1} becomes wider and more intense, indicating overlap between the original O–H hydrogen-bonding signal and additional N–H stretching vibrations from urea-derived groups. The aliphatic C–H bands at 2917 and 2845 cm^{-1} also increase in intensity, consistent with the introduction of methylene bridges from the UF resin.

 © 2026 UMK Publisher. All rights reserved.

In the carbonyl region near 1703 cm^{-1}, an enhanced shoulder and slight shift (or additional absorption) are observed, which can be associated with carbonyl or amide-like C=O/C–N contributions from UF oligomers. The band at ~1599 cm^{-1} is retained but shows a modest change in shape and intensity; it is therefore primarily assigned to aromatic skeletal vibrations (aromatic C=C), with a possible minor contribution from conjugated quinone-like C=O groups. Finally, the feature at 1224 cm^{-1} increases in intensity compared with unmodified HA. This band is best interpreted as an overlap of contributions, including phenolic C–O and in-plane O–H bending, as well as C–N or C–O stretching associated with UF. Accordingly, its assignment should be made with caution (Sari et al. 2021; Sari and Rusdiarso 2022).

Taken together and supported by changes observed in XRD, SEM-EDX (elemental N increase), and altered acidity/pH-stability, these spectral modifications provide consistent evidence that UF has been incorporated into the HA matrix (Basuki et al. 2021b; Sari et al. 2021; Silverstein et al. 2014).

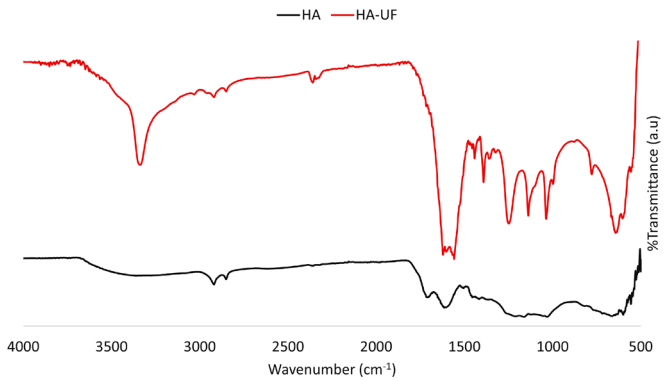


Figure 1: ATR-IR Spectrum of HA and HA-UF

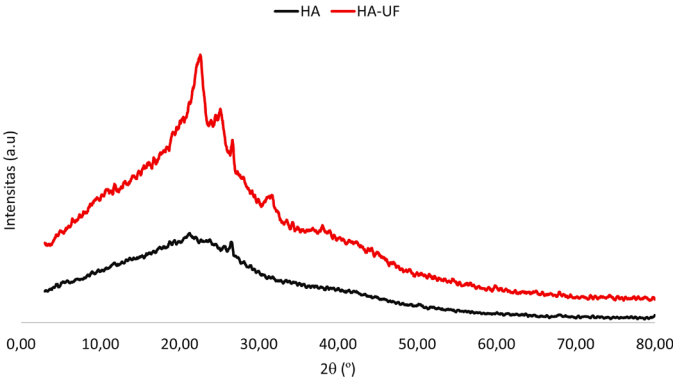


Figure 2: Diffractogram of HA and HA-UF

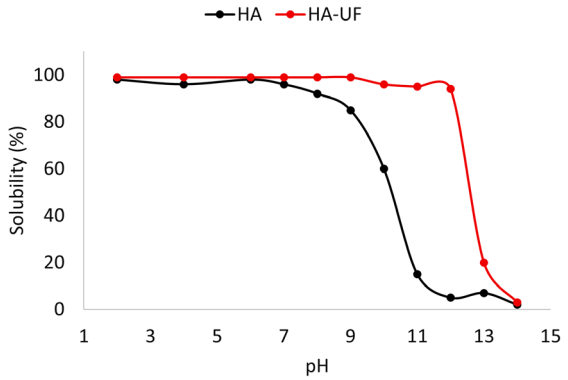


Figure 3: Solid stability of HA and HA-UF in response to pH variation

The interpretation of the ATR-IR spectra of UF modified HA must take into account the substantial band overlap characteristic of humic substances. Direct comparison with the unmodified HA spectrum reveals several changes; however, many of these features occur in regions where multiple functional groups absorb and therefore cannot be considered uniquely diagnostic of UF incorporation.

The broad absorption near ~3400 cm^{-1} becomes slightly more intense after modification, but this region is dominated by O–H stretching from phenolic and carboxylic groups and can broaden further due to hydrogen bonding or adsorbed water. Thus, attributing this feature to N–H stretching from UF is not definitive. The carbonyl band near ~1710 cm^{-1} also exhibits a slight shift and/or increase in intensity. Although this may indicate changes in the local carbonyl environment such as esterification, hydrogen-bond rearrangement, or acid base interactions its assignment solely to amide C=O formation should be made with caution. Definitive evidence of covalent UF HA linkage would require the clear appearance of amide I (~1650 cm^{-1}) and amide II (~1540 cm^{-1}) bands; however, these features are not distinctly resolved in the spectrum of the modified HA. Several weaker bands (1620, 1441, 1390, and 1248 cm^{-1}) exhibit minor changes in intensity, but these regions overlap extensively with intrinsic HA vibrations (aromatic C=C, CH bending, phenolic C–O). Although these features may indicate altered microstructures or additional C–N/C–O environments, they are not uniquely diagnostic of UF modification (Silverstein et al. 2014).

The XRD pattern of HA (Figure 2) exhibits broad and

 © 2026 UMK Publisher. All rights reserved.

low intensity peaks, reflecting its predominantly amorphous nature. In contrast, HA-UF displays relatively sharper diffraction peaks at 2θ = 21°, 23°, and 25°, suggesting that molecular interactions introduced by UF modification increased the local structural order (Figure 2). Cross-reaction with formaldehyde forms C−N and C−O−C bonds between HA and UF, thus increasing the crystalline phase in HA. Enhancing the crystallinity of the adsorbent material may improve its physical stability, targeted adsorption capacity, and overall performance.

The solubility evaluation across various pH levels (Figure 3) shows that HA-UF exhibits greater stability than unmodified HA, particularly under alkaline conditions, and remains stable up to pH 12. This enhanced stability correlates with the reduced total acidity and modified elemental composition of HA-UF (Table 1). The material shows a total acidity of 349.3 cmol/kg, which is lower than the unmodified material due to the UF modification. Elemental analysis further supports this transformation (Table 1), with the nitrogen content increasing substantially from 6.85% in HA to 23.46% in HA-UF. This significant increase suggests the incorporation of nitrogen containing functional groups and the formation of additional polymeric structures following UF modification.

The morphology of the samples is presented in the SEM images shown in Figures 4a and 4b. In these micrographs, the UF phase can be distinguished by its brightness and contrast variations. Figure 4b clearly shows brighter regions corresponding to UF-rich areas, illustrating that the UF phase is evenly distributed within the HA matrix. Compared to Figure 4a, which shows the rough and irregular surface characteristic of untreated HA, the HA-UF sample in Figure 4b exhibits a more compact and cohesive morphology. Several smoother, plate-like fragments are visible on the surface, suggesting the development of new polymeric domains following UF modification. In addition, the reduced presence of fine granules and the more consolidated texture observed in Figure 4b indicate that UF may act as a binding agent, partially filling pores and decreasing surface heterogeneity. Overall, these morphological differences are consistent with the incorporation of UF into the HA framework.

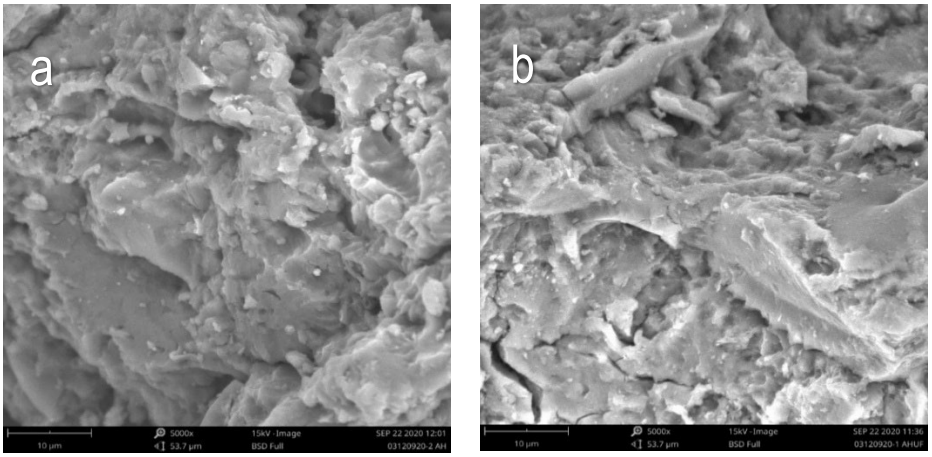


Figure 4: The morphology of (a) HA and (b) HA-UF

Table 1. Characteristic parameters of HA and HA-UF (Total acidity and elemental analysis)

Material	Total Acidity (cmol/kg)	Elemental Analysis (%w/w)		
		C	O	N
HA	549.2	57.60	35.55	6.85
HA-UF	349.3	46.13	30.23	23.46

Conversely, the carbon and oxygen contents in HA-UF decrease, possibly due to interactions between carboxyl groups in HA and the −NH groups of UF. As a result, the reduction in total acidity and the associated changes in chemical structure likely contribute to the enhanced stability of HA-UF under high pH conditions.

3.2 Adsorption Ni(II) by HA-UF

The adsorption performance of Ni(II) by HA-UF is significantly influenced by pH, ionic strength, and surface modification. The Figure 5, which illustrates the effect of pH on Ni(II) adsorption, shows a distinct trend: at low pH values (pH 2–3), the adsorption of Ni(II) is minimal due to the high concentration of H^+ ions that protonate the active functional groups (–COOH, –OH, –NH) on the HA-UF surface, preventing Ni(II) from binding. As the pH increases toward near-neutral conditions (around pH 5–6), the functional groups become progressively deprotonated, leading to an increase in negative surface charge and enhanced electrostatic attraction

 © 2026 UMK Publisher. All rights reserved.

toward Ni^{2+} ions (Z. Liu et al. 2025). This leads to a significant improvement in adsorption efficiency (Wang and Guo 2020a). Beyond pH 6, the adsorption capacity slightly decreases or stabilizes, which may be attributed to the formation of $Ni(OH)_2$ precipitates that reduce the availability of free Ni(II) ions in solution (Guo et al. 2025; Shiver and Atkins 2009; Wei et al. 2022). This behavior aligns with natural geochemical processes, in which pH is a key factor controlling the solubility and mobility of metals in soil and water systems.

Importantly, the speciation of nickel in aqueous solution is strongly pH-dependent. Under acidic conditions (pH 1–3), Ni^{2+} predominantly exists as free hydrated ions, such as $[Ni(H_2O)_6]^{2+}$. As the pH increases, hydrolysis begins, leading to the formation of species such as $NiOH^+$ and $Ni(OH)_2(aq)$, and eventually to the precipitation of $Ni(OH)_2(s)$ at pH values above approximately 8. The shift from free ions to hydroxide complexes reduces the concentration of adsorbable Ni^{2+} in solution, which explains the slight decrease in adsorption efficiency at alkaline pH (Guo et al. 2025; Shiver and Atkins 2009; Wang and Guo 2020a).

The adsorption isotherm data for Ni(II) on both HA and HA-UF demonstrate a marked improvement in performance following urea-formaldehyde modification (Table 2). According to the Langmuir model, the maximum adsorption capacity (b) increased from 1.899×10^{-4} mol/g (~11.145 mg/g) for HA to 3.682×10^{-4} mol/g (~21.612 mg/g) for HA-UF. This increase suggests enhanced active site availability on HA-UF, likely due to the incorporation of nitrogen-rich functional groups during UF modification. The high R^2 values confirm that the adsorption process follows a monolayer adsorption mechanism on a homogenous surface, typical of the Langmuir model (Wang and Guo 2020a).

The Freundlich model, which describes heterogeneous and potentially multilayer adsorption, also indicates an increase in adsorption capacity, with B values rising from 2.182×10^{-2} mol/g for HA to 8.886×10^{-2} mol/g for HA-UF. However, the corresponding R^2 values are lower than those obtained for the Langmuir model, suggesting that the Langmuir isotherm provides a better fit to the experimental data (Wang and Guo 2020a). Both materials exhibit n values of approximately 2, indicating favorable adsorption. These results further support the conclusion that HA-UF offers a more effective surface environment for Ni(II) uptake compared to unmodified HA.

Table 2. Ni(II) Adsorption Isotherm Parameters on HA and HA-UF

Materials	Langmuir Model				Freundlich Model		
	b ($\times 10^{-4}$ mol/g)	K_L (L/mol)	E (kJ/mol)	R^2	B ($\times 10^{-2}$ mol/g)	n	R^2
HA	1.899	47.401	22,35	0,9955	2.182	2.000	0.7714
HA-UF	3.682	20.242	20,24	0,9991	8.886	2.003	0.8552

The adsorption energy was calculated using the following equation, where *E* (kJ/mol) represents the monolayer adsorption energy:

$$E = -RT \ln K_L \qquad (5)$$

Here, R is the universal gas constant and T is the absolute temperature. The Langmuir adsorption constant (K_l) reflects the affinity between the adsorbent surface and the adsorbate; a higher K_l value indicates stronger binding and a greater tendency for adsorption at low solute concentrations (Basuki et al. 2021b; Jery et al. 2024; Sari et al. 2021).

Based on Table 2, the K_L value for Ni(II) adsorption onto HA (47.401 L/mol) is significantly higher than that for HA-UF (20.242 L/mol). This indicates that pristine humic acid (HA) exhibits a stronger affinity toward Ni(II) ions compared to the ultrafiltered humic acid (HA-UF). The higher K_l value of HA suggests that Ni(II) ions interact more favorably with the available functional groups on HA, such as carboxylate and phenolic moieties, which are well known to form stable surface complexes with divalent metal ions (Basuki et al. 2021a; Hutama et al. 2025).

In contrast, the lower K_L value observed for HA-UF implies a reduced adsorption affinity, which may be attributed to changes in surface chemistry or molecular structure induced by the ultrafiltration process, such as partial loss or redistribution of high-affinity functional sites (Langmuir 1916, 1918; Sari et al. 2021). This trend is consistent with the calculated adsorption energies, which indicate that HA exhibits a higher adsorption energy than HA-UF, suggesting stronger Ni(II) surface interactions on HA. Overall, the higher value for HA implies that Ni(II) binding is energetically stronger on unmodified HA than on HA-UF, consistent with the Langmuir assumption of monolayer adsorption on specific active sites.

The calculated adsorption energies (E) of 22.35 kJ/mol for HA and 20.24 kJ/mol for HA–UF fall within the intermediate adsorption energy range, typically reported to span approximately 20–80 kJ/mol. According to (Basuki, Yusnaidar, and Rusdiarso 2018; Bjørklund et al. 2020; Foo and Hameed 2010; Tran et al. 2017). Adsorption energies within this range generally indicate interactions stronger than simple van der Waals forces and may involve ion-exchange processes, outer sphere or partially inner-sphere

 © 2026 UMK Publisher. All rights reserved.

complexation, as well as other mixed mechanisms (Stevenson 1994). However, although these values suggest interactions stronger than weak physisorption, they do not constitute definitive evidence of true chemisorption. Therefore, the interpretation should be made with appropriate caution.

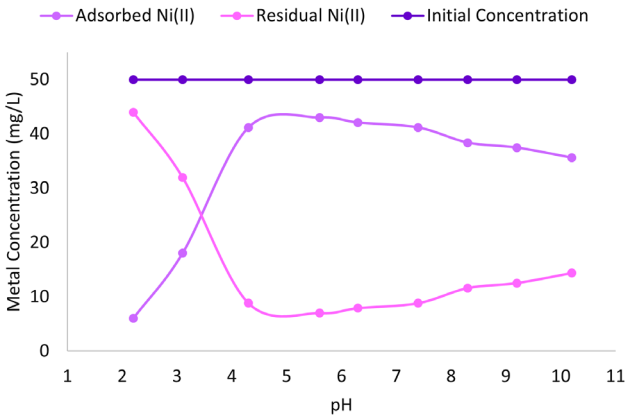


Figure 5: Effect of pH on Ni(II) sorption

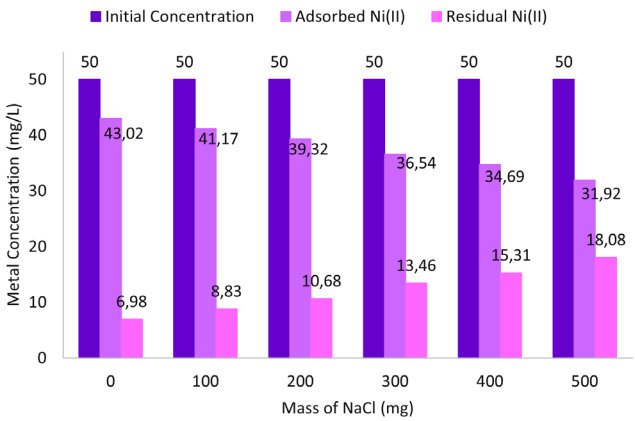


Figure 6: Effect of ionic strength on Ni(II) sorption

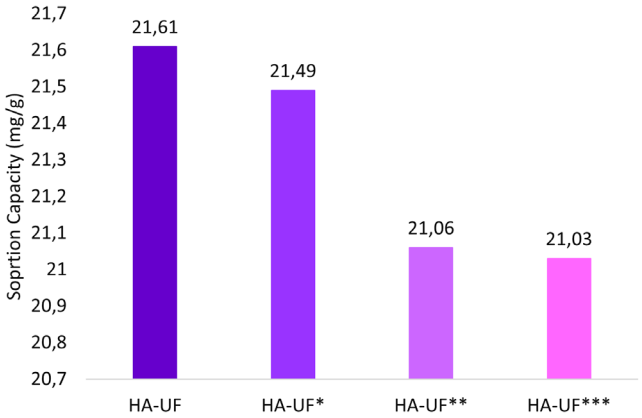


Figure 7: Effect of ionic strength on sorption capacities of HA-UF

The adsorption energy of HA (22.35 kJ/mol) is slightly higher than that of HA-UF (20.24 kJ/mol). If adsorption energy is taken as a proxy for interaction strength, this indicates that HA alone exhibits marginally stronger binding to Ni(II). The small difference of approximately 2 kJ/mol may fall within the typical uncertainty associated with isotherm model fitting (e.g., Dubinin Radushkevich or Temkin models) and therefore cannot be used to support strong claims of improved bonding strength following UF modification. In this context, the enhanced adsorption performance of HA-UF is more plausibly attributed to an increase in the number or accessibility of active sites reflected in the higher adsorption capacity rather than to a substantial change in the intrinsic binding energy per site (Hutama et al. 2025).

Assignments involving –COOH, –OH, and nitrogen-containing groups as Ni(II) binding sites should also be supported with direct evidence. This includes correlating ATR peak shifts (e.g., vC=O, vO–H, amide I/II if UF contributes amide linkages), stability of pH, or elemental analysis. In the absence of supporting evidence, mechanistic claims regarding the involvement of specific functional groups should be considered tentative. Accordingly, although UF modification may enhance the overall adsorption capacity, the calculated energy values suggest that the intrinsic chemical affinity toward Ni(II) does not increase substantial

Figure 6 demonstrates the effect of ionic strength, as represented by increasing concentrations of NaCl. Here, a clear inverse relationship is observed between the NaCl dose and Ni(II) adsorption. As the NaCl mass increases, the adsorbed Ni(II) concentration decreases significantly, while the residual concentration increases. This suggests that Na^{+} ions compete with Ni^{2+} for the same adsorption sites on the HA-UF surface. In addition, increased ionic strength compresses the electrical double layer (Sari et al., 2021; Wei et al., 2022), thereby reducing the electrostatic attraction between HA-UF and Ni(II).

 © 2026 UMK Publisher. All rights reserved.

Figure 7 illustrates the sorption capacity of Ni(II) by HA-UF in the presence of increasing concentrations of NaCl. The control sample (HA-UF) without added NaCl exhibits the highest sorption capacity at 21.61 mg/g. As the NaCl increases, a progressive decline in sorption capacity is observed, down to 21.03 mg/g at the highest concentration.

This trend can be explained by the effect of ionic strength. As the NaCl concentration increases, Na^+ ions compete with Ni^{2+} for the same active adsorption sites on the HA-UF surface, particularly negatively charged functional groups such as COO and O. In addition, higher ionic strength compresses the electrical double layer, thereby weakening electrostatic interactions between the adsorbent and the target metal ions. Together, these effects result in reduced adsorption efficiency (Drahansky et al., 2023; Li et al., 2024; Wang et al., 2025). Therefore, the observed decrease in Ni(II) sorption capacity with increasing NaCl concentration further confirms the roles of electrostatic and ion-exchange mechanisms in the HA-UF adsorption process.

3 Kinetic Sorption Ni(II) by HA-UF

In the pseudo-first-order model (Table 3), the rate constant k_1 increased from 0.018 min^{-1} for HA to 0.027 min^{-1} for HA-UF, while the equilibrium adsorption capacity (q_e) showed a slight increase from 3.736×10^{-4} mol/g to 3.806×10^{-4} mol/g. The R^2 value for HA (0.9948) was higher than that for HA-UF (0.9686), suggesting that the model describes the adsorption kinetics of HA more accurately than those of HA-UF. Nevertheless, the R^2 values remain relatively high for both materials, indicating a reasonably good overall fit.

This trend is consistent with the calculated adsorption energies, which show that HA has a higher adsorption energy than HA-UF, further supporting stronger Ni(II)–surface interactions on HA.

Table 3. Adsorption kinetic parameters of Ni(II) on HA and HA-UF

Materials	Pseudo-first-order			Pseudo-second-order		
	R^2	k_1 (min^{-1})	qe (mol/g)	R^2	k_2 (g/mol·min)	qe (mol/g)
HA	0.9948	0.018	3.736×10^{-4}	0.9477	2.537×10^{-2}	5.028×10^{-4}
HA-UF	0.9686	0.027	3.806×10^{-4}	0.9964	2.328×10^{-2}	5.374×10^{-4}

In contrast, the pseudo-second-order (Table 3) model produced even higher R^2 values 0.9477 for HA and 0.9964 for HA-UF which suggests that this model describes the adsorption behavior more accurately, particularly for HA-UF. The pseudo second order rate constant (k_2) slightly decreased from 2.537×10^{-2} g/mol·min for HA to 2.328×10^{-2} g/mol·min for HA-UF. However, the equilibrium adsorption capacity (q_e) increased from 5.028×10^{-4} mol/g to 5.374×10^{-4} mol/g, indicating improved adsorption capacity for HA-UF. The better fit of the pseudo second order model, particularly for HA-UF, suggests that Ni(II) adsorption may involve chemisorption related mechanisms, such as electron sharing or exchange between Ni(II) and functional groups on the adsorbent surface (Hutama et al. 2025). This interpretation is consistent with the chemical characteristics of HA and HA-UF, which contain abundant oxygen- and nitrogen-containing functional groups capable of interacting strongly with metal ions.

Table 4. Effect of ionic strength on Ni(II) kinetic rate sorption

NaCl (mg)	Pseudo-second-order		
	k_2 (g/mol·min)	qe (mol/g)	R^2
0	2.328×10^{-2}	5.374×10^{-4}	0.9964
100	1.523×10^{-2}	4.804×10^{-4}	0.9928
200	2.419×10^{-2}	4.694×10^{-4}	0.9897
300	1.132×10^{-2}	4.391×10^{-4}	0.9959

Table 4 shows the effect of increasing ionic strength, represented by NaCl concentrations (0–300 mg), on the sorption behavior of Ni(II) ions onto HA-UF, analyzed using the pseudo-second-order kinetic model. The data show a clear decreasing trend in both the adsorption rate constant (k_2) and the equilibrium adsorption capacity (q_e) with increasing NaCl dosage. However, the R^2 values remain high (≥ 0.98), indicating that the pseudo second order model continues to provide a good fit under varying ionic strength conditions.

At 0 mg NaCl, the adsorption rate constant (k_2) is highest at 2.328×10^{-2} g/mol·min, with an equilibrium capacity (q_e) of 5.374×10^{-4} mol/g. As NaCl concentration increases both k_2 and q_e decrease consistently, reaching the lowest values at 300 mg: $k_2 = 1.132 \times 10^{-2}$ g/mol·min and $q_e = 4.391 \times 10^{-4}$ mol/g. This suggests that Na^+ ions compete with Ni^{2+} for active binding sites on the HA-UF surface, thereby reducing the effective adsorption of Ni(II). In addition, increased ionic strength compresses the electrical double layer surrounding the adsorbent, which weakens electrostatic interactions between Ni(II) and the negatively charged functional groups of HA-UF (Sari and Rusdiarso 2022).

These observations are consistent with established adsorption theory, which explains that high ionic strength suppresses ion adsorption by shielding the adsorbent surface

 © 2026 UMK Publisher. All rights reserved.

and introducing competitive cations in solution. The presence of background electrolytes like NaCl can significantly impact ion sorption processes, particularly in systems governed by electrostatic and ion-exchange mechanisms.

Based on the calculated adsorption capacity, kinetic behavior, and the proposed molecular interaction scheme shown in the figure, the interaction of Ni(II) ions with the HA-UF surface is likely dominated by specific surface complexation rather than simple physical adsorption. Ni(II) ions are present in solution mainly as hydrated species (e.g., $[Ni(H_2O)_6]^{2+}$) (Shiver and Atkins 2009), which approach the HA-UF surface and interact with oxygen- and nitrogen-containing functional groups such as carboxylate, phenolic hydroxyl, and amide/amine groups, as illustrated in the proposed structure (Figure 8 and Figure 9).

The good agreement with the pseudo-second-order kinetic model suggests that the adsorption rate may be influenced by chemical interactions, indicating the possible formation of relatively strong Ni(II)–surface bonds (Hutama et al. 2025; Rusdiarso and Basuki 2020). As illustrated in the figure, Ni(II) may form inner-sphere complexes, in which partial dehydration occurs and coordination bonds are established between Ni(II) and donor atoms (O or N) on HA-UF. In parallel, outer-sphere complexation may also take place, in which hydrated Ni(II) ions are retained through electrostatic attraction and hydrogen bonding between coordinated water molecules and HA-UF functional groups (Bhati, Rao, and Kumar 2025; Z. Liu et al. 2025; Zhang et al. 2019). This statement was illustrated by Figure 8 and 9.

In addition, Figure 9 illustrates the role of ionic competition and ion-exchange mechanisms, in which Ni(II) ions replace exchangeable cations (e.g., Na^+ or H^+) initially associated with negatively charged sites on HA-UF (Basuki et al. 2021b; B. Liu et al. 2025; Z. Liu et al. 2025; Sari et al. 2021). This exchange is facilitated by the higher charge density and stronger complexation tendency of Ni(II), which contributes to the observed adsorption capacity.

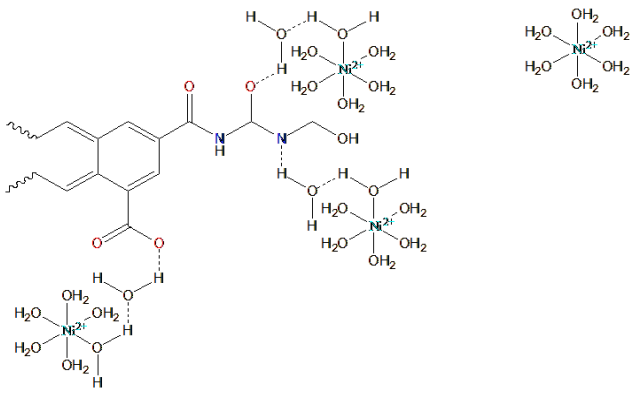


Figure 8. Illustration of Ni HA-UF interaction

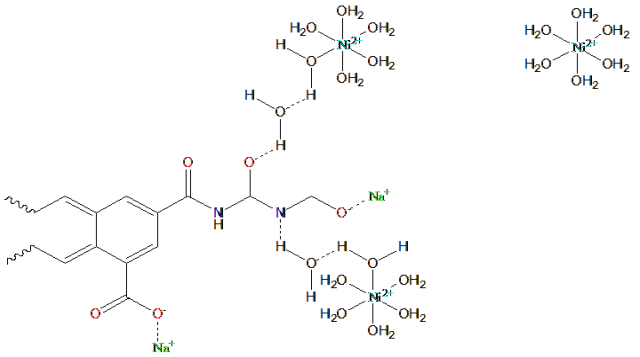


Figure 9. Illustration of Competition Ni with Na at HA-UF

Overall, the combined interpretation of adsorption capacity, kinetic results, and the proposed molecular interaction model confirms that Ni(II) adsorption onto HA-UF is governed by chemisorption involving coordination bonding and ion exchange, supported by electrostatic interactions and hydrogen bonding, leading to stable Ni(II)–HA-UF surface complexes.

3.4 Geochemical interpretation of Ni(II) adsorption mechanisms

A geochemical perspective provides deeper insight into the adsorption mechanisms governing Ni(II) interactions with HA and HA-UF and helps clarify how solution chemistry and surface functionality control metal-binding efficiency (Ali et al. 2025; Drozhzhin et al. 2025; Zakirova et al. 2025). The pH-dependent adsorption behavior observed in this study reflects fundamental geochemical controls on metal speciation and ligand reactivity. Under acidic conditions, Ni(II) predominantly exists as hydrated cations, such as $[Ni(H_2O)_6]^{2+}$ (Shiver and Atkins 2009), while the HA-UF surface remains highly protonated, thereby limiting complex formation (Sari and Rusdiarso 2022; Shiver and Atkins 2009).

This pattern is consistent with natural organic matter reactivity in peat and sediment systems, where proton competition suppresses metal ligand binding at low pH (Hayes, Mylotte, and Swift 2017; Stevenson 1994; Xue et al. 2024). As the pH approaches neutrality, deprotonation of carboxylate, phenolic, and amine groups increases the negative surface charge, thereby promoting the formation of inner sphere complexes through ligand exchange reactions. Geochemical modeling studies indicate that this pH range coincides with the stability field of dissolved Ni^{2+} prior to significant hydrolysis and precipitation, which explains the observed maximum adsorption around pH 5–6 (Drozhzhin et al. 2025; Sari and Rusdiarso 2022).

The modification of HA with urea-formaldehyde

 © 2026 UMK Publisher. All rights reserved.

introduces additional amide and amine groups, enriching the adsorbent with nitrogen-containing coordination sites that mimic natural humification processes, where N-functionalization increases metal affinity (Isakov 2021). The increase in nitrogen content from 6.85% to 23.46% in HA-UF suggests the incorporation of nitrogen containing functional groups that may participate in chelate like interactions with Ni(II). Such interactions are consistent with a chemisorption related mechanism, as inferred from the adsorption energy values (>20 kJ/mol), although these values alone do not provide definitive proof of true chemisorption (Foo and Hameed 2010). Similar enhancements in metal-binding capacity have been reported for nitrogen-enriched humic substances and crosslinked biopolymers (Basuki et al. 2021a; Ngatijo et al. 2021). The semi crystalline features observed in HA-UF by XRD suggest the development of relatively more ordered microdomains, which may facilitate metal ligand coordination and contribute to improved sorption performance and structural stability.

Ionic strength plays a crucial geochemical role by influencing the competition between Ni^{2+} and background electrolytes and modulating electrostatic interactions (Drozhzhin et al. 2025; Sari and Rusdiarso 2022). Increasing NaCl concentration resulted in reduced adsorption capacity and slower adsorption rates, indicating that Na^{+} ions compete with Ni^{2+} for negatively charged sites on the HA-UF surface. This observation is consistent with findings in soil and aquatic geochemistry, where high ionic strength conditions reduce the affinity of heavy metals for humic substances due to cation competition and compression of the electrical double layer. Such effects are particularly relevant in natural systems and in real wastewater matrices that contain elevated electrolyte concentrations (Santosa, Siswanta, and Sudiono 2017; Wang et al. 2023; Yang et al. 2019; Zakirova et al. 2025).

Importantly, the persistence of pseudo-second-order kinetics across different ionic strengths suggests that the underlying adsorption mechanism is still dominated by chemisorption, although competitive interactions influence mass transfer and accessibility to binding sites (Santosa et al. 2017; Wang and Guo 2020b). This finding aligns with geochemical studies indicating that, although ionic strength influences the rate and extent of adsorption, it does not fundamentally alter the nature of metal ligand bonding unless processes such as precipitation or mineral surface interactions become dominant (Liang et al. 2021; B. Liu et al. 2025).

Overall, the adsorption behavior of Ni(II) on HA-UF is consistent with geochemical principles governing metal mobility and retention in natural peat, soil, and sediment systems. The interplay of pH-controlled ligand reactivity, ionic competition, and the enhanced functional complexity of HA-UF suggests that this material effectively mimics natural organic matter while offering improved structural stability and metal-binding capacity (Liang et al. 2021). Understanding these geochemical mechanisms strengthens the relevance of HA-UF for practical applications in wastewater treatment, particularly in environments with fluctuating pH and complex ionic backgrounds that closely resemble natural geochemical conditions.

4. CONCLUSION

The application of a geochemical approach to modify humic acid derived from Riau peat with urea-formaldehyde (HA-UF) proved effective in enhancing Ni(II) adsorption through structural and functional transformations. The adsorption performance of HA-UF, governed by pH, ionic strength, and reaction kinetics, reflects geochemical interaction patterns commonly observed in natural systems.

ACKNOWLEDGEMENT

The authors thank the Universitas Gadjah Mada for financing this work through the RTA 2020 Programs (Grant Number: 607/UN1/DITLIT/DIT-LIT/PT/2020).

REFERENCES

Ali, Ismat H., Malak F. Alqahtani, Nasma D. Eljack, Sawsan B. Eltahir, Makka Hashim Ahmed, and Abubakr Elkhaleefa. 2025. "Experimental and Machine Learning Modelling of Ni (II) Ion Adsorption onto Guar Gum : Artificial Neural Network (ANN) and K-Nearest Neighbor (KNN) Comparative Study." *Polymers* 17(2791):1–20.

Basuki, Rahmat, Bambang Rusdiarso, Sri Juari Santosa, and Dwi Siswanta. 2021a. "Magnetite-Functionalized Horse Dung Humic Acid (HDHA) for the Uptake of Toxic Lead(II) from Artificial Wastewater." *Adsorption Science & Technology* 2021(5523513):1–15.

Basuki, Rahmat, Bambang Rusdiarso, Sri Juari Santosa, and Dwi Siswanta. 2021b. "Magnetite-Functionalized Horse Dung Humic Acid (HDHA) for the Uptake of Toxic Lead(II) from Artificial Wastewater." *Adsorption Science and Technology* 2021. doi: 10.1155/2021/5523513.

Basuki, Rahmat, Sri Juari Santosa, and Bambang Rusdiarso. 2017. "The Novel Kinetics Expression of Cadmium (II) Removal Using Green Adsorbent Horse Dung Humic Acid (Hd-Ha)." in *AIP Conference Proceedings*. Vol. 1823. American Institute of Physics Inc.

Basuki, Rahmat, Yusnaidar Yusnaidar, and Bambang Rusdiarso. 2018. "Different Style of Langmuir Isotherm Model of Non-Competitive Sorption Zn(II) and Cd(II) onto Horse Dung Humic Acid (HD-HA)." in *AIP Conference Proceedings*. Vol. 2026. American Institute of Physics Inc.

Bhati, Surbhi, Richa Rao, and Mukesh Kumar. 2025. "Effect of Humic Acid Application Methods on Growth , Flowering , and Yield of African Marigold (Tagetes Erecta L .) Cv . Pusa Narangi Gainda." 28(10):122–33.

Bjørklund, Geir, Petro Oliinyk, Roman Lysiuk, Md Shiblur Rahaman, Halyna Antonyak, Iryna Lozynska, Larysa Lenchyk, and Massimiliano Peana. 2020. "Arsenic Intoxication: General Aspects and Chelating Agents." *Archives of Toxicology* 94(6):1879–97. doi: 10.1007/s00204-020-02739-w.

Charazińska, S., P. Lochyński, and E. Burszta-Adamiak. 2021. "Removal of Heavy Metal Ions Form Acidic Electrolyte for Stainless Steel Electropolishing via Adsorption Using Polish Peats." *Journal of Water Process Engineering* 42:102169. doi: https://doi.org/10.1016/j.jwpe.2021.102169.

Charazińska, Sylwia, Ewa Burszta-Adamiak, and Paweł Lochyński. 2022. *Recent Trends in Ni(II) Sorption from Aqueous Solutions Using Natural Materials*. Vol. 21.

Drahansky, Martin, M. .. Paridah, Amin Moradbak, A. .. Mohamed, Folahan abdulwahab taiwo Owolabi, Mustapha Asniza, and Shawkataly H. .. Abdul Khalid. 2023. "Heavy Metals in Wastewater Effluent: Causes, Effects and Removal Technologies." Pp. 1–7 in *Trace Metals in the Environment.*

 © 2026 UMK Publisher. All rights reserved.

IntechOpen.
Drozhzhin, Nikita A., Olga Yu Ponomareva, Ilya I. Vinogradov, Genrikh V Serpionov, Abubakir Kanet, Daria V Nikolskaya, and Tatiana N. Vershinina. 2025. "Nickel (II) Based Metal-Organic Framework Consolidated on Nanofibers Modified Track-Etched Membrane for Dye Removal." *Eurasian Journal of Chemistry* 3(119):118–28.
Foo, K. Y., and B. H. Hameed. 2010. "Insights into the Modeling of Adsorption Isotherm Systems." *Chemical Engineering Journal* 156(1):2–10. doi: 10.1016/j.cej.2009.09.013.
Freundlich, Herbert. 1907. "Über Die Adsorption in Lösungen." *Zeitschrift Für Physikalische Chemie* 57U(1):385–470. doi: 10.1515/zpch-1907-5723.
Genchi, Giuseppe, Alessia Carocci, Graziantonio Lauria, Maria Stefania Sinicropi, and Alessia Catalano. 2020. "Nickel: Human Health and Environmental Toxicology." *International Journal of Environmental Research and Public Health* 17(3). doi: 10.3390/ijerph17030679.
Guo, Yaling, Gang Wang, Xiaoyan Zhu, Yongpeng Sun, and Liang Dai. 2025. "Adsorption of Ni(II) from Aqueous Solution by Wheat Straw Modified with Mercaptopropionyl Functional Groups." *Langmuir* 41(8):5488–5503. doi: 10.1021/acs.langmuir.4c05125.
Hayes, Michael H. B., Rosaleen Mylotte, and Roger S. Swift. 2017. *Humin: Its Composition and Importance in Soil Organic Matter*. Vol. 143.
Ho, Y. S., and McKay. G. 1995. "A Comparison of Chemisorption Kinetic Model Applied to Pollutant Removal on Various Sorbents." *Trans IChemE.* 76(Part B).
Hutama, Raihansyah Raja, Audrey Nur Aisyah, Azzahra Sandri, Mayang Fauziah Putri, Sultan Napoleon, Yusuf Bramastya Apriliyanto, and Nugroho Adi Sasongko. 2025. "Adsorption Ni (II) on Magnetic Fulvic Acid-Chitosan : Kinetics and Isotherm Study." *Sorption Studies* 1(1):13–20. doi: https://doi.org/10.55749/ss.v1i1.79.
Isakov, V. A. 2021. "Research on the Adsorption of Heavy Metal Ions from Model Solutions by Humic Acids Isolated from Sapropel." *IOP Conference Series: Earth and Environmental Science* 852(1):12039. doi: 10.1088/1755-1315/852/1/012039.
Jery, Atef El, H. Alawamleh, Mustafa Humam Sami, Hussein Abdullah Abbas, S. S. Sammen, Amimul Ahsan, M. Imteaz, Abdallah Shanableh, M. Shafiquzzaman, Haitham Osman, and Nadhir Al-Ansari. 2024. "Isotherms, Kinetics and Thermodynamic Mechanism of Methylene Blue Dye Adsorption on Synthesized Activated Carbon." *Scientific Reports*.
Lagergren, S. 1898. "Kungliga Svenska Vetenskapsakademiens." *Handlingar* 24(4):1–39.
Langmuir, Irving. 1916. "The Constitution and Fundamental Properties of Solids and Liquids." *Journal of the American Chemical Society* 38(11):2221–95. doi: 10.1021/ja02268a002.
Langmuir, Irving. 1918. "The Adsorption of Gases on Plane Surfaces of Mica." *Journal of the American Chemical Society* 40(9):1361–1403. doi: 10.1021/ja01269a066.
Li, Ke Jin, Alfin Kurniawan, Georgios E. Christidis, Jia Yong He, and Chun Hui Zhou. 2024. "Interfacial Interactions Controlling Adsorption of Metal Cations on Montmorillonite." 109(4):633–55. doi: doi:10.2138/am-2022-8834.
Liang, Suu Yan, Wen Sheng Lin, Chan Po Chen, Chen Wuing Liu, and Chihhao Fan. 2021. "A Review of Geochemical Modeling for the Performance Assessment of Radioactive Waste Disposal in a Subsurface System." *Applied Sciences (Switzerland)* 11(13). doi: 10.3390/app11135879.
Liu, Bei, Iso Christl, Sarah Benware, Zhongying Wang, and Joel A. Pedersen. 2025. "Association of the Ionizable Organic Compound Lamotrigine with Dissolved Humic Acid: Mechanistic Insights and Modeling Optimization." *Environmental Science & Technology* 59(42):22842–51. doi: 10.1021/acs.est.5c06863.
Liu, Zhaoli, Jiahui Fu, Qianfen Xiao, Wei-Xian Zhang, and Airong Liu. 2025. "Influence of Humic Acid on Nanoscale Zerovalent Iron Reaction in Oxic Water: Structural Evolution, (•)OH Generation, and As(III) Sequestration." *Environmental Science & Technology* 59(41):22262–72. doi: 10.1021/acs.est.5c07323.
Ngatijo, Ngatijo, Nurul Gusmaini, Restina Bemis, and Rahmat Basuki. 2021. "Adsorpsi Methylene Blue Pada Nanopartikel Magnetit Tersalut Asam Humat: Kajian Isoterm Dan Kinetika." *CHEESA: Chemical Engineering Research Articles* 4(1):51. doi: 10.25273/cheesa.v4i1.8433.51-64.
Ohalete, M. N., and A. V Popoola. 2019. "Urea-Formaldehyde Resins Synthesis, Modification and Characterization." *IOSR Journal of Applied Chemistry (IOSR-JAC* 12(8):19–25. doi: 10.9790/5736-1208011925.
Rusdiarso, Bambang, and Rahmat Basuki. 2020. "Stability Improvement of Humic Acid as Sorbent through Magnetite and Chitin Modification." *Jurnal Kimia Sains Dan Aplikasi* 23(5):152–59. doi: 10.14710/jksa.23.5.152-159.
Santosa, Sri Juari, Dwi Siswanta, and Sri Sudiono. 2017. *Dekontaminasi Ion Logam Dengan Biosorben Berbasis Asam Humat, Kitin, Dan Kitosan*. Yogyakarta: Gadjah Mada University Press.
Santoso, Uripto Trisno, Dewi Umaningrum, Utami Irawati, and Radna Nurmasari. 2010. "Immobilization of Humic Acid on Chitosan Using Protected Cross-Linking Reaction Method and Its Application as Sorbent for Pb(II), Cd(II), and Cr(III)." *Indonesian Journal of Chemistry* 8(2):177–83. doi: 10.22146/ijc.21620.
Sari, Meidita Kemala, Rahmat Basuki, and Bambang Rusdiarso. 2021. "Adsorption of Pb(II) from Aqueous Solutions onto Humic Acid Modified by Urea-Formaldehyde: Effect of PH, Ionic Strength, Contact Time and Initial Concentration." *Indonesian Journal of Chemistry* 21(6):1371–88.
Sari, Meidita Kemala, and Bambang Rusdiarso. 2022. "The Study of PH and Ionic Strength on Ni(II) and Pb(II) Sorption Using Humic Acid-Urea Formaldehyde (AHUF)." *Indonesian Journal of Chemical Science and Technology (IJCST)* 5(1):31–41. doi: 10.22146/ijc.64600.
Shiver, Shriver, and Peter Atkins. 2009. *Inorganic Chemistry*. Fifth Edit. New York: Oxford University Press.
Silverstein, R. M., F. X. Webster, D. J. Kiemle, and D. L. Bryce. 2014. *Spectrometric Identification of Organic Compounds*. 8th ed. John Wiley & Sons.
Spark, K. M., J. D. Wells, and B. B. Johnson. 1997. "The Interaction of a Humic Acid with Heavy Metals." *Australian Journal of Soil Research* 35(1):89–101. doi: 10.1071/S96008.
Stevenson, Frank J. 1994. *Humus Chemistry: Genesis, Composition, Reactions*. New York: John Wiley & Sons.
Tran, Hai Nguyen, Sheng-Jie You, Ahmad Hosseini Bandegharaei, and Huan-Ping Chao. 2017. "Mistakes and Inconsistencies Regarding Adsorption of Contaminants from Aqueous Solutions : A Critical Review." *Water Research* 120:88–116. doi: 10.1016/j.watres.2017.04.014.
Wang, Baoying, Jingming Lan, Chunmiao Bo, Bolin Gong, and Junjie Ou. 2023. "Adsorption of Heavy Metal onto Biomass-Derived Activated Carbon: Review." *RSC Advances* 13(7):4275–4302. doi: 10.1039/d2ra07911a.
Wang, Jianlong, and Xuan Guo. 2020a. "Adsorption Isotherm Models : Classification, Physical Meaning, Application and Solving Method." *Chemosphere* 258:127279. doi: 10.1016/j.chemosphere.2020.127279.
Wang, Jianlong, and Xuan Guo. 2020b. "Adsorption Kinetic Models: Physical Meanings, Applications, and Solving Methods." *Journal of Hazardous Materials* 390(November 2019):122156. doi: 10.1016/j.jhazmat.2020.122156.
Wang, Yangxin, Xiandi Wu, Xunzhang Li, Chang Zhang, Xinru Lv, Zhufeng Zhang, Xusheng Wang, Hongqi Shi, Feng Yang, and Huaixia Zhao. 2025. "Covalently Crosslinked Carboxymethyl Chitosan Beads Containing SiO2 and Ionic Polymer for Efficient Adsorptive Removal of Methylene Blue." *International Journal of Biological Macromolecules* 294:139441. doi: https://doi.org/10.1016/j.ijbiomac.2024.139441.
Wei, Zhanxi, Yidan Zhu, Yuanyuan Wang, Zefeng Song, Yuanzhao Wu, Wenli Ma, Yongxia Hou, Wenqing Zhang, and Yuesuo Yang. 2022. "Influence of Soil Colloids on Ni Adsorption and Transport in the Saturated Porous Media: Effects of PH, Ionic Strength, and Humic Acid." *Applied Sciences (Switzerland)* 12(13). doi: 10.3390/app12136591.
Xue, Shuwen, Yunhu Hu, Keji Wan, and Zhenyong Miao. 2024. "Exploring Humic Acid as an Efficient and Selective Adsorbent for Lead Removal in Multi-Metal Coexistence Systems: A Review." *Separations* 11(3):1–21. doi: 10.3390/separations11030080.
Yang, Yi jin, Bin Wang, Xu jing Guo, Chang wu Zou, and Xian dong Tan. 2019. "Investigating Adsorption Performance of Heavy Metals onto Humic Acid from Sludge Using Fourier-Transform Infrared Combined with Two-Dimensional Correlation Spectroscopy." *Environmental Science and Pollution Research* 26(10):9842–50. doi: 10.1007/s11356-019-04445-2.
Zakirova, E. Yu., A. M. Aimaletdinov, M. N. Mansurova, and A. G. Malanyeva. 2025. "Features of the Influence of Humic Acids to Aquaculture." *Fisheries*.
Zhang, Yanhong, Changqing Zhu, Fuqiang Liu, Yuan Yuan, Haide Wu, and Aimin Li. 2019. "Effects of Ionic Strength on Removal of Toxic Pollutants from Aqueous Media with Multifarious Adsorbents: A Review." *Science of the Total Environment* 646:265–79. doi: 10.1016/j.scitotenv.2018.07.279.

 © 2026 UMK Publisher. All rights reserved.